Particularly interesting Cys-His-rich protein is highly expressed in human intracranial aneurysms and resists aneurysmal rupture

YU-TAO PENG[1], XIANG-EN SHI[1], ZHI-QIANG LI[1], XIN HE[2] and YU-MING SUN[2]

[1]Department of Neurosurgery, Fu Xing Hospital; [2]Department of Neurosurgery, Sanbo Brain Hospital,
Capital Medical University, Beijing 100038, P.R. China

Abstract. Particularly interesting Cys-His-rich protein (PINCH) has several biological functions in cancer development, invasion and metastasis in malignant cells, and the expression of PINCH is upregulated in several cancer types, including breast cancer, gastric adenocarcinoma and rectal cancer. However, the contribution of PINCH to human cerebral aneurysms remains largely unknown. Therefore, the significance of PINCH expression in cerebral aneurysm growth and rupture was examined in the present study. The protein expression levels of alpha-smooth muscle actin, osteopontin (OPN), matrix metalloproteinase (MMP) 9 and PINCH were evaluated using immunohistochemistry and western blot analyses. The results demonstrate that the protein expression levels of OPN, MMP9 and PINCH in the unruptured intracranial aneurysm (UA) and ruptured intracranial aneurysm (RA) groups were markedly higher than those of the control group, whereas OPN and PINCH expression levels were decreased in the RA group compared to those of the UA group. In addition, there was a strong correlation between PINCH and tumor size (r=0.650 and P=0.0026), as well as between PINCH and OPN (r=0.639 and P=0.0033) in the unruptured cerebral aneurysms. However, the correlation between PINCH and tumor size (r=0.450 and P=0.1393) and between PINCH and OPN (r=0.366 and P=0.2426) revealed no obvious difference in the ruptured cerebral aneurysms. In conclusion, PINCH was highly expressed in the UAs, which may be a critical factor for preventing aneurysmal rupture. Moreover, PINCH may facilitate intracranial aneurysm progression, at least partially, through the activation of extracellular signal-regulated kinase signaling and the suppression of c-Jun N-terminal kinase signaling.

Correspondence to: Dr Xiang-En Shi, Department of Neurosurgery, Fu Xing Hospital, Capital Medical University, 20A Fu Xing Men Wai Da Jie, Beijing 100038, P.R. China
E-mail: xeshimed@hotmail.com

Introduction

Intracranial aneurysms (IAs) are relatively common vascular abnormalities of the cerebrum and are the third leading cause of cerebrovascular accidents, accounting for ~3% in the general population (1). Currently, the incidence and operations of IAs have significantly increased, and IA-associated clinical manifestations, such as intracranial hypertension and hemorrhage, are considered to have a diameter of ≥0.6 cm for patients with increasing risk of rupture, which is associated with significant morbidity and mortality (2,3). Notably, subarachnoid hemorrhage remains lethal in up to 65% of cases, and significantly disables 50% of those who survive (4). Complex open surgical repair and endovascular approaches have proven to be a good and potent alternatives to open repair of these aneurysms for older and high-risk patients as well as for aneurysms with optimal morphological suitability (5). However, intervention therapy has the risk of developing a neurological injury (6-8). Nevertheless, the advances in effective therapy for IAs have been limited due to inherited pathogenic pathways remaining obscure. Therefore, identification of the molecular mechanism for the IAs is required in order to develop an effective treatment.

Particularly interesting Cys-His-rich protein (PINCH), which is composed of 5 LIM domains arrayed in tandem, is expressed in an ubiquitous manner in early embryonic development and adult tissues and has been suggested to be important in processes as diverse as migration, cell adhesion, differentiation, proliferation and survival (9,10). Functional studies have revealed that PINCH loss-of-function leads to embryonic lethality and displays an abnormal epiblast polarity, impaired cavitation, detachment of primitive endoderm (PrE) and severe apoptosis of the PrE (11,12). PINCH-1 promotes B-cell lymphoma (Bcl)-2-dependent survival signalling and inhibits c-Jun N-terminal kinase (JNK)-mediated apoptosis in the PrE (13). Although the function of PINCH remains unknown, increasing numbers and accumulating evidence indicates that PINCH has been correlated with cancer development, invasion and metastasis in malignant cells, including breast cancer (14), pseudomyxoma peritonei (15), gastric adenocarcinoma (16) and rectal cancer (17). For example, PINCH is demonstrated to protect tumor cells from apoptosis by increasing the activity of the pro-survival protein extracellular signal-regulated kinase (ERK)1/2 and Akt (18). In breast cancer cells, Ras

suppressor-1 induces apoptosis through the suppression of PINCH-1, and the integrin-linked kinase/PINCH/α-parvin (IPP) complex as a therapeutic target is downregulated in the chelidonine-treated MDA-MB-231 cell line (14,19). To the best of our knowledge there is no literature available regarding the association between PINCH abnormal expression and IAs.

In the present study, an association between PINCH and tumor size was revealed, and PINCH was highly expressed in IAs (including unruptured and ruptured aneurysms), in which it was predominantly localized to the lumen. Furthermore, the present study sought to determine the regulatory events associated with the expression of PINCH in ruptured and unruptured human cerebral aneurysms. Moreover, the levels of PINCH were demonstrated to be significantly higher in unruptured compared to ruptured aneurysms as observed by immunohistochemistry and western blotting. In addition, the rupture of aneurysms was associated with the expression of PINCH in the cerebral aneurysms.

Materials and methods

Patients and specimens. A total of 31 IAs (including 19 unruptured and 12 ruptured cerebral aneurysms) were collected from Fu Xing Hospital Affiliated to Capital Medical University (Beijing, China) between Jan 2008 and June 2014. All the patients recruited in the present study were not subjected to preoperative radiotherapy or chemotherapy and were diagnosed with IAs based on histopathological evaluation by digital subtraction angiography (DSA), as previously described (20). The control specimens were 5 intracranial cerebral arteries obtained from patients who underwent surgery. All of the tissue samples collected were immediately stored in liquid nitrogen for western blot analysis or fixed in 10% formalin for immunohistochemical staining. Human samples were obtained with written informed consent from all patients. In addition, the study was approved by the Ethics Committee of the Fu Xing Hospital Affiliated to Capital Medical University (Beijing, China).

Histomorphology and immunohistochemistry. Formalin-fixed and paraffin-embedded tumor tissues were cut into 4 μm sections, which were stained with hematoxylin and eosin (H&E) and visualized under a Leica DM 2500 microscope (Leica Microsystems, Inc., Buffalo Grove, IL, USA).

The 5 control artery and 31 aneurysm samples were immunohistochemically evaluated using anti-human alpha-smooth muscle actin (α-SMA; ab5694; 1:200; Abcam, Cambridge, MA, USA), osteopontin (OPN; sc-20788; 1:100; Santa Cruz Biotechnology, Inc., Santa Cruz, CA, USA), matrix metalloproteinase (MMP) 9 (ab73734; 1:200; Abcam) and PINCH (sc-136299; 1:50, Santa Cruz Biotechnology, Inc.). Tissues embedded in paraffin were cut into 4-μm sections, mounted on glass slides and stained using indirect immunoperoxidase (P0203; Beyotime Institute of Biotechnology, Haimen, China). The paraffin sections were then baked in an oven at 65°C for 24 h, then dewaxing to water, and were rinsed with PBS three times (5 min each time). The sections that were washed well were placed in the EDTA buffer for microwave antigen retrieval, boiled, then low heat (100°C) to boil after an interval of 10 min. Following cooling, the sections were washed with PBS 3 times. They were then placed in 3% hydrogen peroxide solution and incubated at room temperature for 10 min, with the purpose of blocking any endogenous peroxidase. These were then washed with PBS 3 times, and blocked with 5% bovine serum albumin (BSA; ST023; Beyotime Institute of Biotechnology) for 20 min after drying (close charge). Following the removal of the BSA solution, each section was incubated with 50 μl anti-α-SMA, anti-OPN, anti-MMP9 and anti-PINCH primary antibodies overnight at 4°C, and then washed with PBS 3 times. Following the removal of PBS solution, each slice was incubated with 50-100 μl goat anti-rabbit IgG (A0208) and goat anti-mice IgG (A0216; both 1:5,000; both Beyotime Institute of Biotechnology) secondary antibodies at 4°C for 50 min, then washed thrice with PBS, and each slice was added to 50-100 μl freshly prepared DAB solution with the help of a microscope in order to observe color. After washing, the sections were counterstained with hematoxylin, rinsed with tap water, dehydrated and mounted. Six sections were randomly selected with no overlapping area (magnification, x200), were observed and photographed. The tissue with brown color (except for the tissue edges) were regarded as α-SMA, OPN, MMP9 and PINCH positive. Image Pro-Plus 6 software (Media Cybernetics, Inc., Rockville, MD, USA) was used for the analysis. The integrated optical density (IOD) was respectively measured for the tumor tissues of immunohistochemical positive staining. The higher the IOD, the higher the expression of the corresponding protein and the lower the expression of the corresponding protein was.

Western blot analysis. Tumor tissues were homogenized and NP-40 buffer (P0013F; Beyotime Institute of Biotechnology) was used to extract them, followed by 5-10 min of boiling and centrifugation at 7,200 x g for 15 min at 4°C in order to obtain the supernatant. A 10% SDS-PAGE gel was used to separate samples containing 50 μg protein, which were then transferred onto nitrocellulose membranes (Bio-Rad Laboratories, Inc., Hercules, CA, USA). Following saturation with 5% (w/v) non-fat dry milk in Tris-buffered saline and 0.1% (w/v) Tween 20 (TBST), the membranes were incubated with the following antibodies: PINCH, OPN, Bcl-2 (sc-56015; 1:2,000), Bcl-2-associated X protein (Bax; sc-20067; 1:2,000), caspase3 (sc-271759; 1:1,000), JNK (sc-137018; 1:500), p-JNK (sc-293136; 1:500), cyclin B1 (sc-7393; 1:1,000), cyclin D1 (sc-70899; 1:1,000), CDC2 (sc-137035; 1:1,000), ERK (sc-514302; 1: 2,000), p-ERK (sc-101761; 1:1,000,), p38 (sc-4315; 1:1,000) and p-p38 (sc-101758; 1:500; all Santa Cruz Biotechnology, Inc.), α-SMA and MMP9 (ab73734; 1:1,000; both Abcam) at 4°C overnight. Following three washes with TBST, the membranes were incubated with goat anti-rabbit IgG and goat anti-mice IgG (both 1:5,000) secondary antibodies conjugated to 800CW Infrared IRDye, including donkey anti-goat IgG and donkey anti-mouse IgG at a dilutions of 1:10,000-1:20,000. After a 1 h incubation at 37°C, the membranes were washed three times with TBST and the blots visualized by the Odyssey Infrared Imaging System (LI-COR Biotechnology, Lincoln, NE, USA). The signals were assessed densitometrically (Odyssey Application Software, version 3.0) and were normalized in order to correct for unequal loading using the mouse monoclonal anti-β-actin antibody (AP0060; 1:1,000; Bioworld Technology, Inc., St. Louis Park, MN, USA).

Statistical analysis. All the data were expressed as the mean ± standard deviation. The statistical analyses were performed using the SPSS 13.0 statistical software package (SPSS, Inc., Chicago, IL, USA), and one-way analysis of variance was used to perform comparisons among the different groups. $P<0.05$ was used to indicate a statistically significant difference.

Results

Clinical characteristics of patients with ruptured and unruptured aneurysms. No significant differences were observed in the mean age (48.8 vs. 43.6 years old), gender distribution (men/women, 9:10 vs. 5:7) and location of aneurysm between patients with unruptured and ruptured cerebral aneurysms (Tables I and II). Furthermore, the mean sizes of unruptured and ruptured aneurysms were 24.84 and 12.67 mm, respectively. However, the tumor size in the unruptured aneurysms group was significantly higher compared to that of the ruptured aneurysms group ($P<0.05$).

Histological assessment was performed in the normal control (n=5), unruptured (n=19) and ruptured (n=12) cerebral aneurysms. The size of the IAs was distinguished using DSA, and the size of small, large and giant IAs had a diameter <12, 12-25 and >25 mm respectively (Fig. 1A). Moreover, as shown in Tables I and II, the location of IAs was separated by DSA. In the normal control group, H&E staining demonstrated that organized smooth muscle cells and continuous endothelial cells were arranged in the cerebral vessel wall (Fig. 1B). In IAs, there were layers of discontinuous endothelial cells and scattered smooth muscle cells in unruptured aneurysms (Fig. 1B). Fresh or organizing thrombosis lined the luminal, and an extremely thin thrombosis-lined hypocellular wall was observed in the ruptured aneurysms (Fig. 1B).

Expression of α-SMA, OPN, MMP9 and PINCH in IAs. α-SMA positive cells were densely distributed in the control group. However, the levels of α-SMA were significantly decreased in unruptured ($P<0.05$) and ruptured ($P<0.05$) cerebral aneurysms compared to those of the control group, and no difference in α-SMA was noted between patients with unruptured and ruptured cerebral aneurysms (Fig. 2A and B). Moreover, the protein expression levels of OPN, MMP9 and PINCH (all $P<0.05$) in the UA and RA group were significantly higher than those of the control group (Fig. 2A and B). In addition, the level of MMP9 ($P<0.05$) was significantly increased in the RA compared to the UA group. However, OPN and PINCH levels were decreased in the RA group compared to those of the UA group (both $P<0.05$) (Fig. 2A and B). In general, these results suggested that OPN and PINCH tend to show a higher expression in the unruptured cerebral aneurysms compared to ruptured cerebral aneurysms.

In order to examine whether there was a correlation between PINCH and tumor size as well as between PINCH and OPN, which was measured in tumor tissues from the same individuals. As shown in Fig. 3A, measurements obtained from the same individuals were strongly correlated between PINCH and tumor size ($r=0.650$ and $P=0.0026$) as well as between PINCH and OPN ($r=0.639$ and $P=0.0033$) in the unruptured cerebral aneurysms. However, the correlation between PINCH and tumor size ($r=0.450$, $P=0.1393$) and between PINCH and OPN ($r=0.366$ and $P=0.2426$) revealed no obvious difference in the ruptured cerebral aneurysms (Fig. 3B). Consistent with immunohistochemical methods, the western blot results demonstrated that the protein expression of OPN, MMP9 and PINCH in the UA and RA group was markedly higher than those of the control group (all $P<0.05$), and OPN and PINCH (both $P<0.05$) were significantly decreased in the RA group as compared to those of the UA group. However, protein expression of MMP9 was not changed in the RA group compared to the UA group (Fig. 3C). These results indicated that PINCH was highly expressed in the unruptured IAs, which may be a critical factor for preventing aneurysmal rupture.

Diagram depicting the possible regulation mechanism of PINCH in the tumorigenesis of IAs. There are several molecules that have been demonstrated to interact with PINCH signaling. The function of the ternary complex of IPP as a signalling platform is achieved by directly interacting with factors that function as upstream regulators of numerous different signalling pathways (21). The present study summarized the known binding partners of PINCH signaling, which are important in processes as diverse as cell adhesion, migration, proliferation, differentiation, survival and apoptosis (22,23). The results demonstrated a decrease in the pro-apoptotic proteins Bax and caspase3 and an increase in the anti-apoptotic protein Bcl-2 in the RA and UA groups compared to those of the control group (Fig. 4A). Moreover, the JNK signaling pathway was inhibited in unruptured and ruptured cerebral aneurysms, and JNK and p-JNK protein expression were significantly lower in the RA and UA groups compared to the control groups (Fig. 4A). In addition, the steady-state levels of proteins involved in the cell cycle checkpoint were analyzed. The results revealed that cyclin B1, cyclin D1 and CDC2 were upregulated in the RA and UA groups compared to those of the NC group (Fig. 4A). In order to further investigate the potential mechanism that may be involved in the PINCH-associated progression of IAs, the protein expression levels of ERK1/2, p-ERK1/2, p38 and p-p38 in tumor tissues were examined. Western blotting revealed that the protein expression levels of ERK1/2, p-ERK1/2, p38 and p-p38 were markedly reduced in the RA and UA groups compared with the NC group (Fig. 4A). Due to the main role of JNK and ERK signaling in carcinogenesis and maintenance of common cancers, the dysregulated expression of JNK and ERK signaling also affects the expression of its potential downstream targets, which are responsible for a wide range of biological processes, including cell proliferation and differentiation, cell cycle and survival and apoptosis. Thus, the results of the present study indicated that PINCH may facilitate IA progression, at least partially, through the activation of ERK signaling and the suppression of JNK signaling (Fig. 4B).

Discussion

Functional studies reveal that the interaction of PINCH1 with integrin-linked kinase (ILK) is a prerequisite in order to locate both proteins to integrin-mediated adhesion sites and to prevent their proteasome-mediated degradation (24,25). Further studies indicate that PINCH1 regulates the cell-matrix, cell polarity and cell-cell adhesion during the implanting of
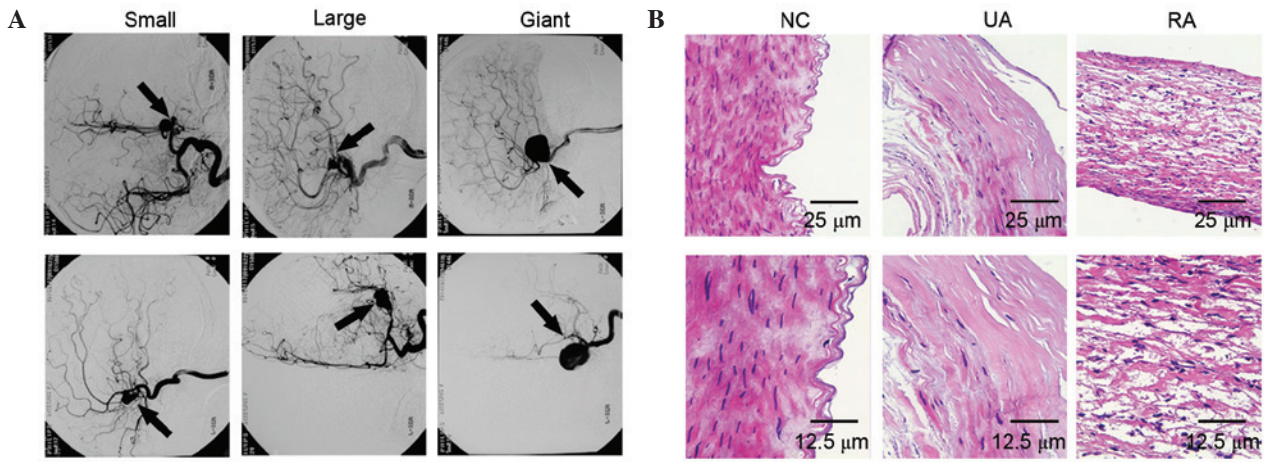
Figure 1. (A) Front view (top) and lateral view (bottom) of the 2D digital subtraction angiogram were applied to depict small (diameter, <12 mm), large (diameter range, 12-25 mm) and giant (diameter, >25 mm) intracranial aneurysms. (B) Pathological staining in NC, UAs and RAs by hematoxylin & eosin staining (top, magnification, x200; scale bar, 25 μm; bottom, magnification, x400; scale bar, 12.5 μm). NC, normal control; UAs, unruptured intracranial aneurysms; RAs, ruptured intracranial aneurysms.
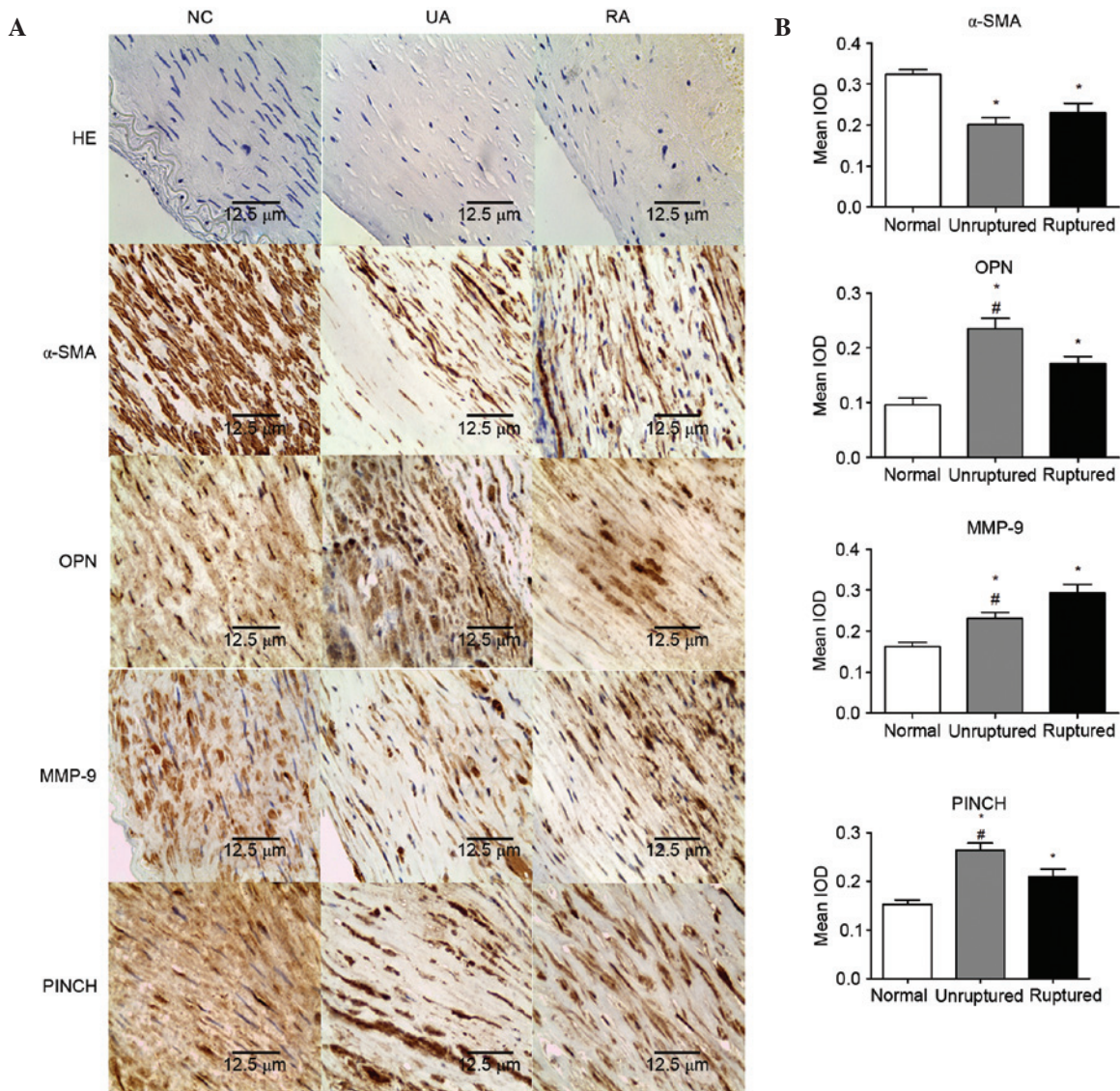

Figure 2. (A) Expression of α-SMA, OPN, MMP9 and PINCH was measured by immunohistochemical staining in the NC, UA and RA (magnification, x400; scale bar, 12.5 μm). (B) IOD was respectively measured for the tumor tissues of immunohistochemical positive staining. Values were expressed as the mean ± standard deviation. *P<0.05 vs. NC group, #P<0.05 vs. RA group. NC, normal control; UA, unruptured intracranial aneurysm; RA, ruptured intracranial aneurysm; HE, hematoxylin and eosin; α-SMA, α-smooth muscle actin; OPN, osteopontin; MMP9, matrix metalloproteinase 9; PINCH, particularly interesting Cys-His-rich protein; IOD, integrated optical density.

Table I. Expression of α-SMA, OPN, MMP9 and PINCH in unruptured aneurysms.

No.	Age	Gender	Location	Size (mm)	α-SMA	MMP9	OPN	PINCH
1	55	M	R-MCA	23	0.201	0.294	0.144	0.287
2	64	M	L-PCA	12	0.307	0.165	0.115	0.228
3	56	M	R-PCA	27	0.158	0.276	0.133	0.186
4	22	M	R-MCA	16	0.231	0.285	0.265	0.273
5	61	M	R-VA	27	0.192	0.253	0.243	0.256
6	6	M	L-PCA	15	0.134	0.221	0.259	0.269
7	51	M	L-VA	22	0.145	0.287	0.184	0.228
8	54	M	R-MCA	12	0.178	0.211	0.213	0.249
9	52	M	L-ICA	35	0.211	0.235	0.356	0.348
10	50	F	L-ICA	12	0.309	0.178	0.174	0.203
11	69	F	L-ICA	30	0.236	0.168	0.194	0.232
12	44	F	L-MCA	34	0.314	0.259	0.184	0.238
13	56	F	L-ICA	7	0.073	0.252	0.283	0.131
14	12	F	L-PCA	30	0.238	0.104	0.236	0.245
15	52	F	R-ICA	40	0.173	0.146	0.189	0.253
16	62	F	R-ICA	15	0.138	0.257	0.324	0.278
17	52	F	R-MCA	40	0.221	0.231	0.341	0.397
18	62	F	R-ICA	25	0.066	0.182	0.195	0.307
19	48	F	R-MCA	50	0.296	0.388	0.429	0.394

M, male; F, female; R, right; L, left; MCA, middle cerebral artery; PCA, posterior cerebral artery; VA, vertebra artery; ICA, internal carotid artery; α-SMA, α-smooth muscle actin; MMP9, matrix metalloproteinase 9; OPN, osteopontin; PINCH, particularly interesting Cys-His-rich protein.

Table II. Expression of α-SMA, OPN, MMP9 and PINCH in ruptured aneurysms.

No.	Age	Gender	Location	Size (mm)	α-SMA	MMP9	OPN	PINCH
1	48	M	R-ACA	9	0.261	0.312	0.172	0.214
2	40	M	L-MCA	20	0.173	0.326	0.224	0.135
3	15	M	L-ACA	6	0.277	0.288	0.108	0.113
4	39	M	L-PICA	7	0.13	0.203	0.192	0.187
5	31	M	R-MCA	7	0.315	0.273	0.094	0.229
6	56	F	R-MCA	5	0.253	0.219	0.149	0.198
7	62	F	R-ICA	15	0.24	0.366	0.197	0.213
8	34	F	L-ICA	20	0.081	0.383	0.146	0.211
9	37	F	L-ICA	5	0.293	0.404	0.139	0.216
10	39	F	L-ICA	15	0.349	0.282	0.188	0.269
11	58	F	L-ICA	30	0.236	0.297	0.253	0.307
12	64	F	L-ICA	13	0.145	0.171	0.186	0.227

M, male; F, female; R, right; L, left; ACA, anterior cerebral artery; MCA, middle cerebral artery; PICA, posterior inferior cerebellar artery; ICA, internal carotid artery; α-SMA, α-smooth muscle actin; MMP9, matrix metalloproteinase 9; OPN, osteopontin; PINCH, particularly interesting Cys-His-rich protein.

mouse embryos (12). Moreover, PINCH1 and ILK function together in controlling cell behavior, including cell shape modulation, motility and survival (12,24). Expression profiles and roles of PINCH in tumor tissues have been previously reported (15,17-19). However, the exact role of PINCH signaling in IA progression and rupture is not clear yet. Therefore, the

aim of the present study was to investigate the function of PINCH signaling in maintaining the development of IAs and preventing aneurysmal rupture.

In the present study several important observations were made. Initially, the basic expression levels of α-SMA, MMP9, PINCH and OPN in 19 unruptured and 12 ruptured cerebral
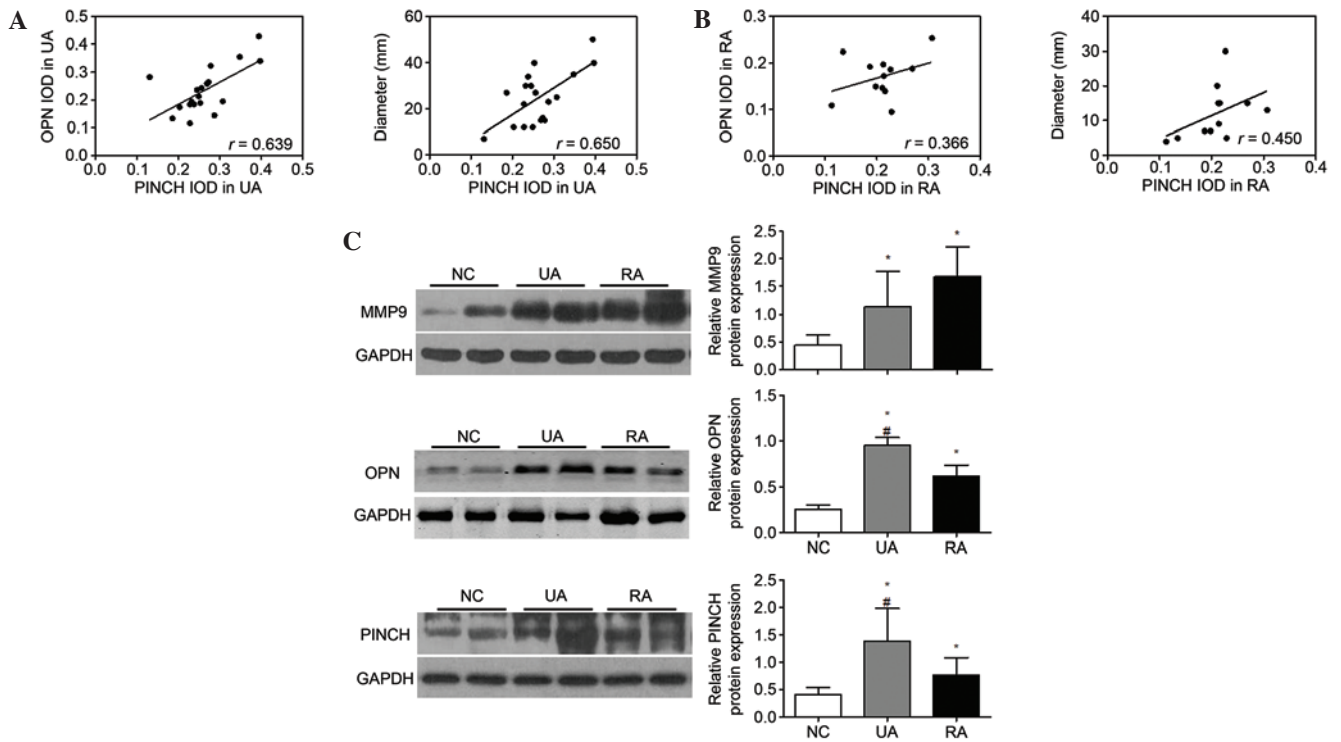
Figure 3. (A) Correlation between PINCH and tumor size as well as PINCH and OPN were measured in the unruptured cerebral aneurysms. (B) The correlation between PINCH and tumor size as well as between PINCH and OPN were measured in the ruptured cerebral aneurysms. (C) Protein expression of MMP9, OPN and PINCH was measured by western blotting in tumor tissues. The values were expressed as the mean ± standard deviation. *P<0.05 vs. NC group, #P<0.05 vs. RA group. OPN, osteopontin; IOD, integrated optical density; UA, unruptured intracranial aneurysm; PINCH, particularly interesting Cys-His-rich protein; RA, ruptured intracranial aneurysm; NC, normal control; MMP9, matrix metalloproteinase 9.
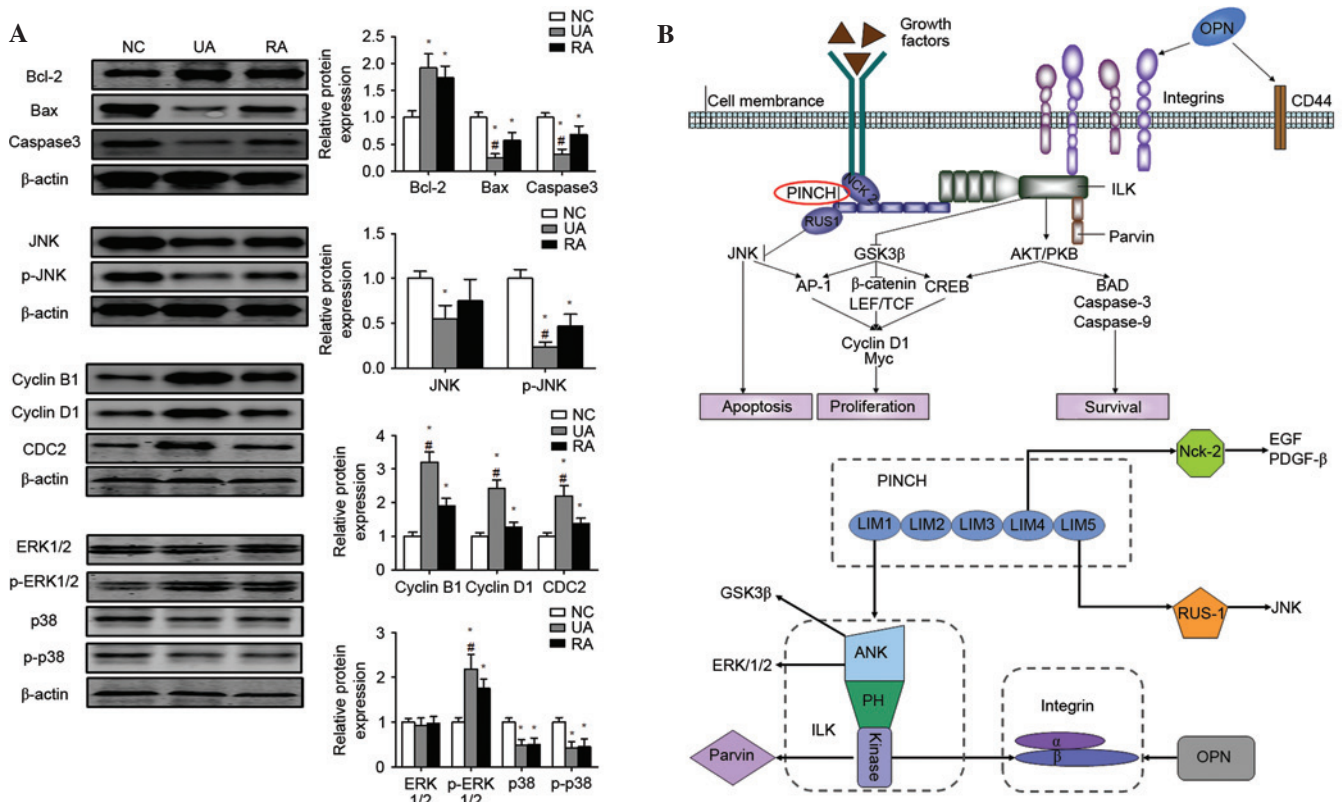

Figure 4. (A) Bcl-2, Bax, caspase3, JNK, p-JNK, cyclin B1, cyclin D1, CDC2, ERK, p-ERK, p38 and p-p38 protein levels were measured by western blotting in tumor tissues. (B) Diagram depicting the possible molecular mechanism of PINCH in the tumorigenesis of intracranial aneurysms. Values were expressed as the mean ± standard deviation, *P<0.05 vs. NC group, #P<0.05 vs. RA group. Bcl-2, B-cell lymphoma-2; Bax, Bcl-2-associated X protein; NC, normal control; UA, unruptured intracranial aneurysm; RA, ruptured intracranial aneurysm; JNK, c-Jun N-terminal kinases; ERK, extracellular signal-regulated kinase; PINCH, particularly interesting Cys-His-rich protein.

aneurysms were studied. Compared to the normal control, the α-SMA, MMP9, PINCH and OPN expression levels were significantly elevated in tumor tissues detected by immuno-histochemical staining and western blotting; however, the expression levels of PINCH and OPN were different between unruptured and ruptured aneurysms. Next, the correlation of PINCH with tumor size and OPN was confirmed, and the linear correlation plot of protein expression between PINCH and tumor size, as well as between PINCH and OPN showed a strong positive correlation in the unruptured aneurysms. Furthermore, the possible molecular mechanism of PINCH in the tumorigenesis of IAs was analyzed and it was revealed that PINCH may facilitate IA progression, at least partially, through the activation of ERK signaling and suppression JNK signaling. This could regulate the downstream regulators, which induce cell proliferation, survival and apoptosis (21).

OPN, which is an important immunomodulator, is a matri-cellular protein that is highly expressed in the aortic wall and was demonstrated to be targeted for cleavage by MMP (26). OPN promotes atherosclerosis through its functions in smooth muscle cell survival, adhesion and migration, and promotes inflammation of carotid plaques in hypertensive patients (27). Furthermore, it mitigates vascular calcification (28) and contributes to the increased amounts of MMP-9 in cardiac and skeletal muscle of mdx mice (29). The present study revealed that the protein levels of MMP9 and OPN were significantly increased in unruptured aneurysms, and the immunohisto-chemical staining was consistent with the with western blot analysis. It is noteworthy that measurements obtained from the same individuals were strongly correlated between PINCH and OPN (r=0.639 and P=0.0033) in the unruptured cerebral aneurysms. However, the correlation between PINCH and OPN (r=0.366 and P=0.2426) showed no obvious difference in the ruptured cerebral aneurysms. These results suggested that PINCH and OPN offered a mechanism of facilitating IA progression, which may be closely associated with resistance of aneurysmal rupture.

Previous studies suggest that PINCH-1 is likely to have a function in the suppression of apoptosis. For example, depletion of PINCH-1 from human HeLa cervical carcinoma cells promotes apoptosis, and an increase of apoptotic endo-dermal cells, mouse embryos and embryonic neural crest cells are observed with PINCH loss-of-function (10,11,18). A prior study suggested that PINCH-1 regulates the anti- and pro-apoptotic pathways and contributes to apoptosis resistance in all types of cancer cells (18). The apoptosis signaling pathway is activated by the loss of PINCH-1, and the level of Bim is significantly increased in response to loss of PINCH-1 in several types of PINCH-1-dependent cancer cells. However, Bim depletion completely blocks the increase of apoptosis induced by the loss of PINCH-1 (18). Moreover, activation of the phosphorylation of the Src family kinase and ERK1/2 is promoted by PINCH-1 (18). In the PrE, PINCH-1 is a pro-survival factor, which prevents apoptosis of PrE cells by modulating two independent signalling pathways; PINCH-1 inhibits JNK-mediated apoptosis by stabilizing the PINCH-1 binding protein RSU-1 and promotes Bcl-2-dependent pro-survival signalling downstream of inte-grins (13). In the present study, a correlation was identified between the activation of ERK signaling and the suppression

of JNK signaling with the expression of PINCH in IAs. The downstream regulators, including anti-apoptotic (Bcl-2), pro-apoptotic proteins (Bax and caspase3) and cell cycle proteins (cyclin B1, cyclin D1 and CDC2) were involved in PINCH-mediated tumorigenesis and progression in IAs.

To the best of our knowledge, this is the first study to report that PINCH is highly expressed in IAs and resists aneurysmal rupture. The study also demonstrated that PINCH may facili-tate IA progression, at least partially, through the activation of ERK and suppression of JNK signaling, which could regulate the downstream regulators including anti- and pro-apoptotic protein and cell cycle proteins.

Acknowledgements

References

1. Chalouhi N, Ali MS, Jabbour PM, Tjoumakaris SI, Gonzalez LF, Rosenwasser RH, Koch WJ and Dumont AS: Biology of intra-cranial aneurysms: Role of inflammation. J Cereb Blood Flow Metab 32: 1659-1676, 2012.
2. Orz Y and AlYamany M: The impact of size and location on rupture of intracranial aneurysms. Asian J Neurosurg 10: 26-31, 2015.
3. Starke RM, Chalouhi N, Jabbour PM, Tjoumakaris SI, Gonzalez LF, Rosenwasser RH, Wada K, Shimada K, Hasan DM, Greig NH, Owens GK and Dumont AS: Critical role of TNF-α in cerebral aneurysm formation and progression to rupture. J Neuroinflammation 11: 77, 2014.
4. Nordon IM, Hinchliffe RJ, Holt PJ, Loftus IM and Thompson MM: Review of current theories for abdominal aortic aneurysm patho-genesis. Vascular 17: 253-263, 2009.
5. Raux M, Patel VI, Cochennec F, Mukhopadhyay S, Desgranges P, Cambria RP, Becquemin JP and LaMuraglia GM: A propensity-matched comparison of outcomes for fenestrated endovascular aneurysm repair and open surgical repair of complex abdominal aortic aneurysms. J Vasc Surg 60: 858-863, 2014.
6. Watanabe Y, Kuratani T, Shirakawa Y, Torikai K, Shimamura K and Sawa Y: Hybrid endovascular repair of a dissecting thora-coabdominal aortic aneurysm with stent graft implantation through the false lumen. J Vasc Surg 59: 264-267, 2014.
7. Wiebers DO, Whisnant JP, Huston J III, Meissner I, Brown RD Jr, Piepgras DG, Forbes GS, Thielen K, Nichols D, O'Fallon WM, Peacock J, Jaeger L, Kassell NF, Kongable-Beckman GL, Torner JC; International Study of Unruptured Intracranial Aneurysms Investigators: Unruptured intracranial aneurysms: Natural history, clinical outcome, and risks of surgical and endo-vascular treatment. Lancet 362: 103-110, 2003.
8. Molyneux AJ, Kerr RS, Birks J, Ramzi N, Yarnold J, Sneade M and Rischmiller J; ISAT Collaborators: Risk of recurrent subarachnoid haemorrhage, death, or dependence and standardised mortality ratios after clipping or coiling of an intracranial aneurysm in the international subarachnoid aneurysm trial (ISAT): Long-term follow-up. Lancet Neurol 8: 427-433, 2009.
9. Li Y, Dai C, Wu C and Liu Y: PINCH-1 promotes tubular epithelial-to-mesenchymal transition by interacting with integrin-linked kinase. J Am Soc Nephrol 18: 2534-2543, 2007.
10. Liang X, Sun Y, Schneider J, Ding JH, Cheng H, Ye M, Bhattacharya S, Rearden A, Evans S and Chen J: Pinch1 is required for normal development of cranial and cardiac neural crest-derived structures. Circ Res 100: 527-535, 2007.
11. Liang X, Zhou Q, Li X, Sun Y, Lu M, Dalton N, Ross J Jr and Chen J: PINCH1 plays an essential role in early murine embryonic development but is dispensable in ventricular cardiomyocytes. Mol Cell Biol 25: 3056-3062, 2005.
12. Li S, Bordoy R, Stanchi F, Moser M, Braun A, Kudlacek O, Wewer UM, Yurchenco PD and Fässler R: PINCH1 regulates cell-matrix and cell-cell adhesions, cell polarity and cell survival during the peri-implantation stage. J Cell Sci 118: 2913-2921, 2005.

13. Montanez E, Karaköse E, Tischner D, Villunger A and Fässler R: PINCH-1 promotes Bcl-2-dependent survival signalling and inhibits JNK-mediated apoptosis in the primitive endoderm. J Cell Sci 125: 5233-5240, 2012.
14. Giotopoulou N, Valiakou V, Papanikolaou V, Dubos S, Athanassiou E, Tsezou A, Zacharia LC and Gkretsi V: Ras suppressor-1 promotes apoptosis in breast cancer cells by inhibiting PINCH-1 and activating p53-upregulated-modulator of apoptosis (PUMA); verification from metastatic breast cancer human samples. Clin Exp Metastasis 32: 255-265, 2015.
15. Andréasson H, Wanders A, Sun XF, Willén R, Graf W, Nygren P, Glimelius B, Zhang ZY and Mahteme H: Histopathological classification of pseudomyxoma peritonei and the prognostic importance of PINCH protein. Anticancer Res 32: 1443-1448, 2012.
16. Zhu ZL, Yan BY, Zhang Y, Yang YH, Wang ZM, Zhang HZ, Wang MW, Zhang XH and Sun XF: PINCH expression and its clinicopathological significance in gastric adenocarcinoma. Dis Markers 33: 171-178, 2012.
17. Holmqvist A, Gao J, Holmlund B, Adell G, Carstensen J, Langford D and Sun XF: PINCH is an independent prognostic factor in rectal cancer patients without preoperative radiotherapy-a study in a Swedish rectal cancer trial of preoperative radiotherapy. BMC Cancer 12: 65, 2012.
18. Chen K, Tu Y, Zhang Y, Blair HC, Zhang L and Wu C: PINCH-1 regulates the ERK-Bim pathway and contributes to apoptosis resistance in cancer cells. J Biol Chem 283: 2508-2517, 2008.
19. Kim O, Hwangbo C, Kim J, Li DH, Min BS and Lee JH: Chelidonine suppresses migration and invasion of MDA-MB-231 cells by inhibiting formation of the integrin-linked kinase/PINCH/α-parvin complex. Mol Med Rep 12: 2161-2168, 2015.
20. Zheng SF, Yao PS, Yu LH and Kang DZ: Keyhole approach combined with external ventricular drainage for ruptured, poor-grade, anterior circulation cerebral aneurysms. Medicine (Baltimore) 94: e2307, 2015.
21. Legate KR, Montañez E, Kudlacek O and Fässler R: ILK, PINCH and parvin: The tIPP of integrin signalling. Nat Rev Mol Cell Biol 7: 20-31, 2006.
22. Wang LY, Tang ZJ and Han YZ: Neuroprotective effects of caffeic acid phenethyl ester against sevofluraneinduced neuronal degeneration in the hippocampus of neonatal rats involve MAPK and PI3K/Akt signaling pathways. Mol Med Rep 14: 3403-3412, 2016.
23. Cui ZW, Xie ZX, Wang BF, Zhong ZH, Chen XY, Sun YH, Sun QF, Yang GY and Bian LG: Carvacrol protects neuroblastoma SH-SY5Y cells against Fe(2+)-induced apoptosis by suppressing activation of MAPK/JNK-NF-kappaB signaling pathway. Acta Pharmacol Sin 36: 1426-1436, 2015.
24. Fukuda T, Chen K, Shi X and Wu C: PINCH-1 is an obligate partner of integrin-linked kinase (ILK) functioning in cell shape modulation, motility, and survival. J Biol Chem 278: 51324-51333, 2003.
25. Zhang Y, Chen K, Guo L and Wu C: Characterization of PINCH-2, a new focal adhesion protein that regulates the PINCH-1-ILK interaction, cell spreading, and migration. J Biol Chem 277: 38328-38338, 2002.
26. Papke CL, Yamashiro Y and Yanagisawa H: MMP17/MT4-MMP and thoracic aortic aneurysms: OPNing new potential for effective treatment. Circ Res 117: 109-112, 2015.
27. Wolak T, Sion-Vardi N, Novack V, Greenberg G, Szendro G, Tarnovscki T, Nov O, Shelef I, Paran E and Rudich A: N-terminal rather than full-length osteopontin or its C-terminal fragment is associated with carotid-plaque inflammation in hypertensive patients. Am J Hypertens 26: 326-333, 2013.
28. Jono S, Peinado C and Giachelli CM: Phosphorylation of osteopontin is required for inhibition of vascular smooth muscle cell calcification. J Biol Chem 275: 20197-20203, 2000.
29. Dahiya S, Givvimani S, Bhatnagar S, Qipshidze N, Tyagi SC and Kumar A: Osteopontin-stimulated expression of matrix metalloproteinase-9 causes cardiomyopathy in the mdx model of Duchenne muscular dystrophy. J Immunol 187: 2723-2731, 2011.